DESIGN OF A MANIPULATOR PROTOTYPE FOR ON-ORBIT MODULE REPLACEMENT

Hu Bingshan, Tang Pin, Chen Meng, Zou Huaiwu, Han Liangliang

Shanghai Institute of Aerospace Systems Engineering, No. 3888, Yuanjiang Road, Minhang District, Shanghai, China ,
Email:hubingshan@gmail.com

ABSTRACT

Performance and lifespan of spacecraft can be enhanced and prolonged by space manipulator's on-orbit service. In this paper, a space manipulator prototype is designed for module on-orbit replacement, and the kinematics model of the manipulator is deduced. Kinematics, dynamics and control algorithm co-simulation model is set up for task simulation. Simulation results show that the manipulator prototype in this paper can complete the module replacement task.

1. INTRODUCTION

In microgravity, high temperature range and high radiation space environments, operating capacity and range of the astronauts are limited, but the space manipulator could work well. So, there are important significances in economic and safety aspects by using space manipulator to replace astronauts completing space operation, and the space manipulator has attracted more and more attention of aerospace department all over the world.

Manipulators putting into orbit application include the Shuttle Remote Manipulator System (SRMS), the Space Station Remote Manipulator System (SSRMS) and the Japanese experiment module manipulator system (JEMRMS). These manipulators' lengths are generally more than 6 meters, and the load capacity are more than 7 tons, even up to hundreds of tons. Their main function is to carry large loads. While the small dexterous space manipulator can achieve high tip control accuracy, so it can complete fine operation, such as small module replacement, pushing button and so on. In this field, the United States, Germany and Japan had carried out in orbit validation, such as ETS-VII, orbital express and so on[1][2][3].

As mentioned before, small dexterous space manipulators can be placed inside the space station cabin, satellite or space exposure platform, to complete fine manipulation tasks independently or assist astronauts do the tasks. In this paper, a small dexterous space manipulator is designed to complete the module replacement task. To verify the feasibility of the robot arm to complete the task, firstly the kinematics model of the robot arm is established, and the task simulation model is set up. The kinematics, dynamics characteristics of the manipulator in the whole task process are simulated and analysed.

2. TASK ANALYSIS

As shown in Fig.1, the dexterous manipulator prototype designed in this paper is mounted on the spacecraft simulator, and the process of completing the module replacement task is as follows: firstly, the dexterous manipulator arm moves and extracts the old module from an old module box, and then the old module is put into the module store. Secondly, a new module is extracted from the module store, and installed into the old module box.

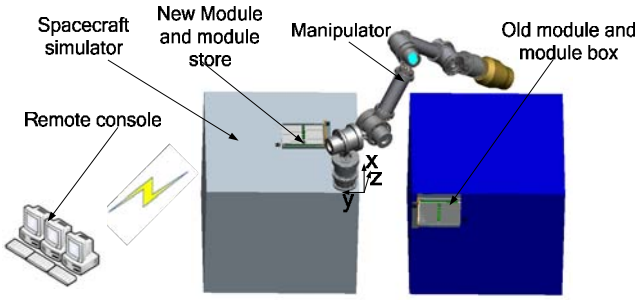

Figure 1 Flowchart of module replacement

The inertial coordinate system origin O_0 is one vertex of the spacecraft simulator. Axis O_0X_0 and axis O_0Y_0 are parallel to the spacecraft's two sides respectively. The axis O_0Z_0 is perpendicular to the installation surface of the module store and deviates from the spacecraft simulator.

The position of the module store in the inertial coordinate system is:

$$\begin{aligned} 400\text{mm} \le X \le 600\text{mm} \\ 200\text{mm} \le Y \le 500\text{mm} \\ 0\text{mm} \le Z \le 185\text{ mm} \end{aligned} \quad (1)$$

The position of the old module in the inertial coordinate system is:

$$\begin{aligned} -185\text{ mm} \le X \le 0\text{ mm} \\ -607\text{ mm} \le Y \le -327\text{ mm} \\ -250\text{ mm} \le Z \le 0\text{ mm} \end{aligned} \quad (2)$$

The dexterous manipulator's reachable space must obtain upon positions as shown in formula (1) and (2).

3. THE SMALL DEXTEROUS MANIPULATOR PROTOTYPE

3.1 PROTOTYPE CONFIGURATION

It is feasible to complete the module replacement task

shown in Fig 2 using a 6 DOF manipulator system, which is composed of shoulder yaw joint, shoulder roll joint, shoulder pitch joint, elbow pitch joint, wrist pitch joint, wrist roll joint, one end effector and manipulator control system. To decrease the envelope size, the elbow joint uses offset layout and other joints use collinear type layout.

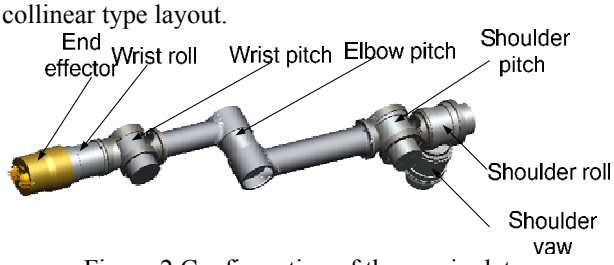

Figure 2 Configuration of the manipulator

3.2 PRECISION ANALYSIS AND DESIGN

To finish the fine operation, control accuracy of the manipulator's tip should be as higher as better. But considering the difficulty of implementation, the absolute position accuracy requirements for the manipulator can be reduced through increasing capture tolerance of the end effector. Considering the arm length, module size and other factors, the capture tolerance of the end effector is designed to 15 mm/1.5°. Moreover, a hand-eye camera and a six axis force sensor are mounted on the end of the arm, and these sensors are used for providing feedback information to improve the accuracy of closed loop control. When the absolute position accuracy is 5 mm and the attitude accuracy is 0.5 °, the manipulator can capture the replaceable module and complete the module replacement task.

The main sources of manipulator end errors are the link length error link twist error, link offset error and joint angle error. Except the joint angle error, the former three errors mainly come from production and assembling, and these errors can offset by calibration. According to manipulator's forward kinematics, the joint angle error's influence on the manipulator's tip precision could be obtained.

Through calculation, when the joint's accuracy is better than 0.05 °, the manipulator's absolute accuracy can be guaranteed. In the design of the joint, we use a harmonic reducer which has a small gap and high precision, and a high accuracy position sensor is used, to meet the requirement of the joint position accuracy.

4. ESTABLISHMENT OF SIMULATION MODEL

4.1 KINEMATICS MODEL

According to the dexterous manipulator's configuration, a link coordinate system is established as shown in Fig.3. DH parameters of the manipulator can be gotten as shown in Tab.1.

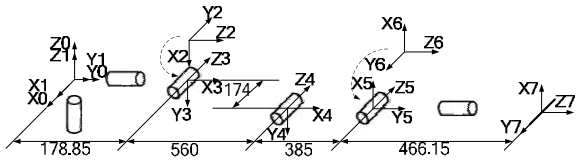

Figure 3 Link coordinate of the manipulator

Table 1 DH parameters of the manipulator

Link i	α_{i-1}	a_{i-1}(mm)	θ_i(Initial angle)	D_i(mm)
1	0°	0	θ1 (0°)	0
2	-90°	0	θ2 (90°)	178.85
3	-90°	0	θ3 (-90°)	0
4	0°	560	θ4 (0°)	-174
5	0°	385	θ5 (-90°)	0
6	-90°	0	θ6 (0°)	0
7	0°	0	0	466.15

The generalized coordinate transformation matrix between two adjacent link i+1 and i is,

$$
\begin{aligned}
{}^{i-1}T_i &= Rot(Z,\theta_i)Trans(0,0,d_i)Trans(a_i,0,0)Rot(X_i,\alpha_i) \\
&= \begin{bmatrix} \cos\theta_i & -\sin\theta_i & 0 & a_{i-1} \\ \sin\theta_i\cos\alpha_{i-1} & \cos\theta_i\cos\alpha_{i-1} & -\sin\alpha_{i-1} & -\sin\alpha_{i-1}d_i \\ \sin\theta_i\sin\alpha_{i-1} & \cos\theta_i\sin\alpha_{i-1} & \cos\alpha_{i-1} & \cos\alpha_{i-1}d_i \\ 0 & 0 & 0 & 1 \end{bmatrix}
\end{aligned} \tag{3}
$$

Substituting the DH parameters in Tab.1 into the Eq (3) respectively, the transformation matrix ${}^{i-1}T_i$ are gotten, and the forward kinematics for the manipulator is,

$$
\begin{aligned}
{}^0T_6 &= \begin{bmatrix} n_x & o_x & a_x & p_x \\ n_y & o_y & a_y & p_y \\ n_z & o_z & a_z & p_z \\ 0 & 0 & 0 & 1 \end{bmatrix} \\
&= {}^0T_1(\theta_1)\,{}^1T_2(\theta_2)\,{}^2T_3(\theta_3)\,{}^3T_4(\theta_4)\,{}^4T_5(\theta_5)\,{}^5T_6(\theta_6)
\end{aligned} \tag{4}
$$

4.2 INVERSE KINEMATICS MODEL

Using the manipulator's inverse kinematics, the demand joint angle θ_i can be derived from the manipulator's tip position and posture $(x, y, z, \alpha, \theta, \beta)$. The transformation matrix of the tip point relative to the base coordinate of the manipulator is,

$$
\begin{aligned}
T_6^0 &= \begin{bmatrix} n_x & o_x & a_x & p_x \\ n_y & o_y & a_y & p_y \\ n_z & o_z & a_z & p_z \\ 0 & 0 & 0 & 1 \end{bmatrix} \\
&= \begin{bmatrix} \mathrm{c}(\beta)\mathrm{c}(\theta) & -\mathrm{c}\beta\,\mathrm{s}\theta & \mathrm{s}\beta & x \\ \mathrm{s}\alpha\,\mathrm{s}\beta\,\mathrm{c}\theta+\mathrm{c}\alpha\,\mathrm{s}\theta & -\mathrm{s}\alpha\,\mathrm{s}\beta\,\mathrm{s}\theta+\mathrm{c}\alpha\,\mathrm{c}\theta & -\mathrm{s}\alpha\,\mathrm{c}\beta & y \\ -\mathrm{c}\alpha\,\mathrm{s}\beta\,\mathrm{c}\theta+\mathrm{s}\alpha\,\mathrm{s}\theta & \mathrm{c}\alpha\,\mathrm{s}\beta\,\mathrm{s}\theta+\mathrm{s}\alpha\,\mathrm{c}\theta & \mathrm{c}\alpha\mathrm{c}\beta & z \\ 0 & 0 & 0 & 1 \end{bmatrix}
\end{aligned} \tag{5}
$$

In Eq (5), *c* refers to *cos*, *s* refers to *sin*. To make Eq (4) equal to Eq (5), using separate variable method, θ_2 and

θ_6 are calculated directly,

$$\theta_6 = a\tan 2(a,b) + a\tan 2(\pm\sqrt{a^2+b^2-d_4^2}, -d_4) \quad (8)$$

$$\theta_2 = a\cos(\mathrm{n}_z \sin(\theta_6) + o_z \cos(\theta_6)) \quad \text{or}$$

$$\theta_2 = -a\cos(\mathrm{n}_z \sin(\theta_6) + o_z \cos(\theta_6)) \quad (9)$$

$$a = n_x p_x + n_y p_y + n_z p_z - d_7 n_z a_z - d_7 n_y a_y - d_7 n_x a_x \quad (10)$$

$$b = o_x p_x + o_y p_y + o_z p_z - d_7 o_z a_z - d_7 o_y a_y - d_7 o_x a_x \quad (11)$$

Substituting θ_2 and θ_6 to Eq (4), the other joint angles can be gotten, and the manipulator's inverse kinematics is established.

4.3 PATH PALNNING ALGORITHM

In the process of extracting or inserting the module, the trajectory of the manipulator's tip must be perpendicular to the module slot. In the other position, there aren't such special requirement and the tip of the manipulator just move from one point to another point freely.

According to the above requirements, in the process of extracting or inserting the module, the path planning algorithm based on the tip position in Cartesian space is used. In the other position, the path planning algorithm based on the position in joint space is used to reduce the amount of calculation.

The flow of the joint space path planning algorithm is as following: firstly, the initial angle θ_{i0} and end angle θ_{if} (i=1，2…6) of each joint is obtained by using the inverse kinematics formulas according to the manipulator tip's starting pose *m1* and ending pose *m2*. It is supposed that every joint has the same rotating time t_f, so in time t, each joint's angle can be gotten according to the five order polynomial interpolation [4][5],

$$\theta_i(t) = a_{0i} + a_{1i}t + a_{2i}t^2 + a_{3i}t^3 + a_{4i}t^4 + a_{5i}t^5 \quad (12)$$

Constraints of the Eq (12) is,

$$\begin{cases} \theta_i(0) = \theta_{0_i} = 0 \\ \theta_i(t_f) = \theta_{f_i} \\ \dot{\theta}_i(0) = 0 \\ \dot{\theta}_i(t_f) = 0 \\ \ddot{\theta}_i(0) = 0 \\ \ddot{\theta}_i(t_f) = 0 \end{cases} \quad (13)$$

Substituting formula (13) to formula (12), we can get joint angle $\theta_i(t)$, which is used for joint position's real time control.

The flow of the Cartesian space path planning algorithm is as following: firstly, the manipulator's pose *x(t)* (*t* refer to time) between the starting pose *m1* and ending pose *m2* is gotten using the five order polynomial interpolation, then each joint's angle $\theta_i(t)$ is obtained by the arm's inverse kinematics formulas, and $\theta_i(t)$ is each joint's control command.

4.4 SIMULATION MODEL

To carry out kinematics, dynamics and control arithmetic co-simulation during the whole module replacement process, the manipulator's inverse kinematics solution program and path planning algorithm is realized using C++ software. The co-simulation model is in Fig.4, in which ZT is path planning module, and FT is inverse kinematics solution module. The dynamics model is established using ADAMS software as showing in Fig. 5. All of these modules are connected by ADMAS Mechanism.

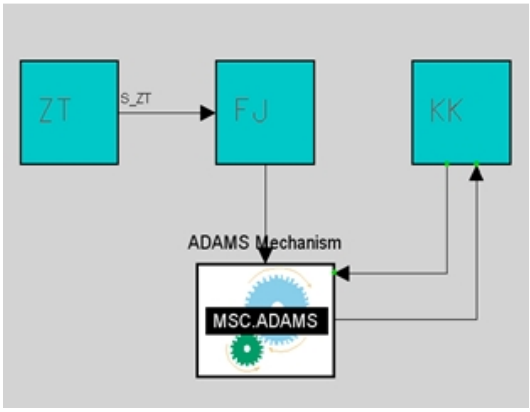

Figure 4 Co-simulation model

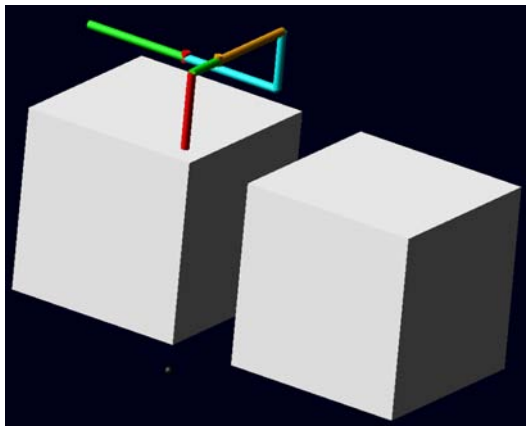

Figure 5 The manipulator's dynamics model

Some hypothesizes are given before simulation: each joint's maximal speed is 0.35°/s, the module's weight is 2 kg, the maximal contact force between the manipulator's tip and the module is 20N.

5. SIMULATION RESULTS

5.1. REACHABLE SPACE ANALYSIS

The manipulator tip's reachable space is analysed by the

kinematics, and its reachable space is as showing in Fig.6. The reachable space is an ellipsoid, whose long axis is 1590 mm, and short axis is 1411.15 mm. It is obvious that the module's position is contained in the reachable space, so the robot arm can reach the old module and the module store.

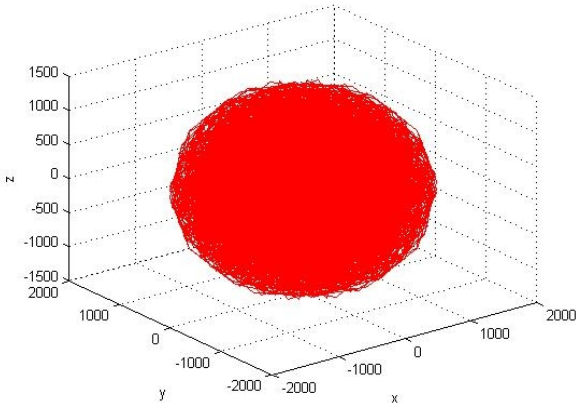

Figure 6 The manipulator's reachable space

5.2. MOTION TRAJECTORY ANALYSIS

The module replace task simulation process is as follows: firstly, the manipulator moves from initial position to the old module's above place, and the manipulator's tip do a linear motion to capture the old module, after that, the manipulator's tip do a linear motion again to the opposite direction to extract the old module. Secondly, the manipulator carrying the old module moves to the above place of the module store, and insert the old module to a slot.

The manipulator tip's trajectory relative to spacecraft simulator is shown in Fig.7. In Fig.7, *mb1* is the manipulator's initial point, *mb2* is the point above the old module, *mb3* is the point where the manipulator capture the old module, *mb4* is the point where the manipulator has extracted the old module, *mb5* is the point of the slot, *mb6* is the point that the manipulator has insert the old module into the slot. From Fig.7, we can find that the path planning algorithm is feasible, and there isn't interference between the manipulator and the spacecraft simulator, so the manipulator has the ability of completing the module replacement task.

5.3. JOINT TORQUE ANALYSIS

In the module replacement task, each joint torque is shown in Figure 7, and the maximum torque is 107.5Nm which appears in the shoulder pitch joint. The maximum torque is smaller than the joint's maximum output torque.

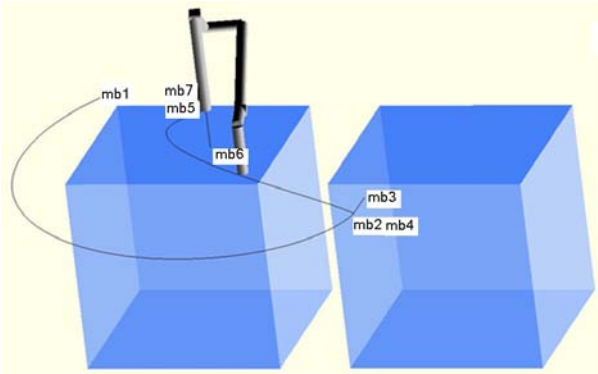

Figure 7 Trajectory relative to spacecraft simulator

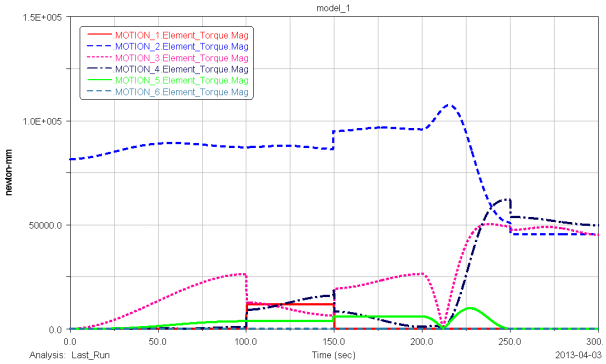

Figure 8 Output torque of each joint during module replacement

6. CONCLUSION

In this paper, a small dexterous manipulator prototype is designed, and its kinematics, dynamics and control co-simulation model is established to analyse the whole module replacement task. Simulation results show that, the module is in the reachable space of the manipulator. There isn't interference between the manipulator and the spacecraft simulator, the path planning algorithm in this paper is feasible. The maximum torque in the replacement process is smaller than the joint's maximum output torque, so the manipulator in this paper has the ability of completing module replacement task.

7. REFERENCES

1. James, F. A., Peter,D. S. (1993). The Development Test Flight of the Flight Telerobotic Servicer: Design Description and Lessons Learned. *IEEE Transactions on Robotics and Automation*. 9(3), 664-674.

2. Carignan, C. (1996). A Decoupling Inverse Kinematics Algorithm for the Ranger Dexterous Manipulator, IEEE Int. Conf. on Robotics and Automation, Minneapolis, United State.

3. LeCroy, J. E., Hallmark, D. S., Howard, R. T. (2007). Effects of Optical Artifacts in a Laser-Based Spacecraft Navigation Sensor, SPIE Conference Proceedings on Sensors and Systems for Space Applications, Bellingham, WA.

4. Landzettel, K., Brunner, B., Hirzinger, G. (1994). The Telerobotic Concepts for ESS. IARP Workshop on Space Robotics, Montreal, Canada.

5. Eckard Settelmeyer, Ralf Hartmann, K. Landzettel, Erich Lehrl, Winfried Oesterlin. (1998). The Experimental Servicing Satellite ESS, 21st ISTS Conference, Omiya, Japan.